Regular Article

HEMATOPOIESIS AND STEM CELLS

A novel role for factor VIII and thrombin/PAR1 in regulating hematopoiesis and its interplay with the bone structure

Anna Aronovich,[1] Yaniv Nur,[1] Elias Shezen,[1] Chava Rosen,[1] Yael Zlotnikov Klionsky,[1] Irit Milman,[1] Liran Yarimi,[1] David Hagin,[1] Gidi Rechavi,[2] Uriel Martinowitz,[3] Takashi Nagasawa,[4,5] Paul S. Frenette,[6] Dalit Tchorsh-Yutsis,[1] and Yair Reisner[1]

[1]Immunology Department, Weizmann Institute of Science, Rehovot, Israel; [2]Cancer Research Center, and [3]The Israel National Hemophilia Center, Sheba Medical Center, Tel Hashomer, Israel; [4]Department of Immunobiology and Hematology, Institute for Frontier, Medical Sciences, Kyoto University, Kyoto, Japan; [5]Japan Science and Technology Agency, Core Research for Evolutional Science and, Technology, Tokyo, Japan; and [6]Institute for Stem Cell and Regenerative Medicine, Albert Einstein College of Medicine, Bronx, NY

Key Points

- The coagulation cascade via the factor VIII/thrombin/PAR1 axis regulates HSC maintenance.
- The coagulation cascade via factor VIII/thrombin/PAR1 axis regulates a reciprocal interplay between HSCs and the dynamic bone structure.

Analysis of hematopoietic stem cells (HSCs) in factor VIII knockout (FVIIIKO) mice revealed a novel regulatory role for the coagulation cascade in hematopoiesis. Thus, HSCs in FVIIIKO mice had reduced proportions of $CD34^{low}$ cells within $Lin^{-}Sca^{+}Kit^{+}$ progenitors, and exhibited reduced long-term repopulating capacity as well as hyper granulocyte–colony-stimulating factor (G-CSF)–induced mobilization. This disregulation of HSCs is likely caused by reduced levels of thrombin, and is associated with altered protease-activated receptor 1 (PAR1) signaling, as PAR1 KO mice also exhibited enhanced G-CSF–induced mobilization. Analysis of reciprocal bone marrow (BM) chimera (FVIIIKO BM into wild-type recipients and vice versa) and the detection of PAR1 expression on stromal elements indicates that this phenotype is likely controlled by stromal elements. Micro–computed tomography analysis of distal tibia metaphyses also revealed for the first time a major impact of the FVIII/thrombin/PAR1 axis on the dynamic bone structure, showing reduced bone:tissue volume ratio and trabecular number in FVIIIKO and PAR1KO mice. Taken together, these results show a critical and novel role for the coagulation cascade, mediated in part by thrombin-PAR1 interaction, and regulates HSC maintenance and a reciprocal interplay between HSCs and the dynamic bone structure. (*Blood*. 2013;122(15):2562-2571)

Introduction

Organ size control during embryonic development or in tissue regeneration in adulthood involves a fine balance between cell growth and proliferation and cell death. This balance is maintained by extrinsic and intrinsic factors.[1]

Recently, we have demonstrated that transplantation of embryonic day 42 (E42) pig embryonic spleen tissue can correct hemophilia A in factor VIII knockout (FVIIIKO) SCID mice.[2] Considering that early attempts to correct hemophilia in humans with adult spleen transplants were associated with fatal graft-versus-host disease (GVHD),[3] the advantage of transplanting embryonic tissue lies in its ability to afford FVIII secretion without any risk for GVHD, as embryonic spleen at this time point is completely devoid of T cells which only arrive at a later gestational age.[2] Using this system, we surprisingly found that a single gene defect in the recipients, namely FVIII, was sufficient to induce significant increase the final size of different transplanted embryonic pig tissues, including pancreas, liver, kidney, and spleen.[4]

We attributed the enhanced size to an imbalance of the host's growth restriction mechanism, which normally resists the tendency of the embryonic pig's tissue implant to grow to its full size. Because of the embryonic origin of the graft, we speculated that the effect is mainly exerted on somatic stem cells residing within the embryonic implant. Such organ-specific somatic stem cells have been previously shown to greatly influence organ growth.[5]

Following this serendipitous discovery, we attempted in the present study to further investigate the mechanism which underlies these findings in a more physiological setting.

An ideal system to test our hypothesis can be afforded by the blood tissue, known to be under tight size control.[6-8] The hematopoietic system is constantly replenished by somatic stem cells, under the guidance of local and systemic growth factors, which determine the total cell number of each blood cell type. During hematopoiesis, lineage-specific growth factors promote the proliferative expansion of progenitor pools, while growth factor deprivation leads to contraction by apoptosis. For example, decreased oxygen tension caused by low red blood cell volume induces expression of the erythroid growth factor Erythropoietin and red blood cell production.[9] Likewise, binding of the megakaryocyte growth

Submitted August 14, 2012; accepted August 13, 2013. Prepublished online as *Blood* First Edition paper, August 27, 2013; DOI 10.1182/blood-2012-08-447458.

A.A. and Y.N. contributed equally to this study.

The publication costs of this article were defrayed in part by page charge payment. Therefore, and solely to indicate this fact, this article is hereby marked "advertisement" in accordance with 18 USC section 1734.

factor thrombopoietin to platelets results in an autoregulation that is inversely related to platelet abundance.[9,10] Such regulatory loops, in which mitogen expression is linked to cell number through a feedback mechanism, likely apply to other adult tissues as well.

In the present study, we found that FVIIIKO mice exhibit imbalance in the hematopoietic stem cell (HSC) pool. This was based on several assays, including staining for cell-surface markers, functional analysis of long-term repopulating (LTR) stem cells, and the exaggerated response of FVIIIKO mice to exogenous granulocyte–colony-stimulating factor (G-CSF) stimulation, known to induce marked splenomegaly both in normal mice and in humans.[11] This imbalance could be potentially mediated by the low levels of thrombin found in these mice. To further address this possibility, we used protease-activated receptor 1 knockout (PAR1KO) mice in which thrombin-PAR1 signaling is aborted. Furthermore, using micro–computed tomography (micro-CT) of the bone tissue we interrogated the role of the FVIII/thrombin/PAR1 axis in regulating the interplay between HSCs and the bone structure.

Materials and methods

Animals

Mice used were 6- to 14-week-old females as specified in "Results." PAR1KO and FVIIIKO mice were purchased from Roscoe B. Jackson Memorial Laboratory (Bar Harbor, ME). PAR1KO was provided after backcrossing at The Jackson Laboratory for >8 generations on a C57BL/6 background. The FVIIIKO strain was provided on a B6129SF2/J background and backcrossed for 8 generations to a C57BL/c background at The Weizmann Institute, using the Jackson polymerase chain reaction screening protocol. GFP-CXCL12 and GFP-Nestin mice were a kind gift of Drs Nagasawa[12] and Frenette.[13] Age- and sex-matched C5BL/6 mice, purchased from Harlan Israel, were used in control experiments, in line with The Jackson Laboratory considerations for choosing controls.

All animals were maintained under conditions approved by the Institutional Animal Care and Use Committee at The Weizmann Institute. All mice were kept in small cages (up to 5 animals per cage) and fed sterile food.

Flow cytometry

Peripheral blood (PB) cells or bone marrow (BM) cells harvested following flushing were examined with different antibodies including the biotinylated lineage antibody cocktail CD3, B220, CD11b, Gr-1, Ter119 (BD Biosciences) as well as Sca-1-PB or Sca-1 phycoerythrin (PE), c-KIT–allophycocyanin or c-KIT PE Cy 5.5, CD34–fluorescein isothiocyanate (FITC) and streptavidin PE-Cy7. For the analysis of stromal cells, anti-CD45 PE, anti-CD31 PE, anti-Ter119 PE, anti-Sca1 PB, anti–platelet-derived growth factor receptor-α (PDGFR-α), and anti-PAR1 (SC-8204) were used as described.

In BM transplantation (BMT) competitive renewal studies, PB cells were stained with anti-CD45.1 FITC and anti-CD45.2 PE antibodies to determine percentage of chimerism. Antibodies were purchased from Bioscience and Biolegend. Data were acquired on an LSRII (BD Biosciences) flow cytometer and analyzed using FlowJo software.

Competitive repopulation assay

B6SJL (CD45.1) recipient mice, at least 11 weeks old, were lethally irradiated (1000 rad) 2 days prior to BMT. Donor mice, 6- to 8-week-old B6SJL (CD45.1) mice with either a C57BL or a FVIII KO counterpart (CD45.2), were sacrificed, and BM single-cell suspension was prepared. Nucleated cells were then counted and mixed in 1:1 or 1:3 ratios and delivered intravenously through the tail vein. Recipient mice were treated with oral Ciprofloxacin delivered through drinking water for 2 weeks posttransplant. Mice were bled every 4 weeks for chimerism analysis by fluorescence-activated cell sorter (FACS).

G-CSF mobilization

Mobilization was achieved by treating mice with 250 μg/kg G-CSF (Neupogen) administered subcutaneously once daily for 5 to 7 days. After G-CSF treatment, PB or BM cells were collected and subjected to flow cytometry analysis.

TGA

The thrombin generation assay (TGA) is performed using 96-well plates and a Thermo Electron Fluorometerkan (Fluoroskan FL) equipped with 390/460 nanometer filter. In this method, FXI-deficient plasma is used and the coagulation is triggered in the presence of 1 pM tissue factor and 4 μM phospholipids. The reaction of thrombin generation at 37°C is initiated upon addition of the buffer containing the fluorescent substrate and Ca^{+2}. C57BL/6 and FVIIIKO plasma were tested and the amount of generated thrombin (nM) in every sample was calculated using instrument software (Thrombinoscop BV). The final thrombin amount is obtained by reducing the background value from the sample value.

ELISA measurements

SDF-1 mouse-specific enzyme-linked immunosorbent assay (ELISA) was purchased from R&D Systems. BM serum (1/2 mL) was collected from flushed femurs and tibias via centrifugation and supernatant segregation. ELISA was performed according to the manufacturer's protocol. Osteocalcin measurement was performed using the Mouse Osteocalcin ELISA kit (Biomedical Technologies). Frozen plasma samples were used.

Histochemistry

Paraffin sections (4 μM) were xylene deparaffinized and rehydrated. Histochemistry included hematoxylin/eosin (H&E) and Serius Red staining.

For immunohistochemical labeling, frozen sections of femurs were prepared and the following antibodies were used: rabbit anti-mouse PAR1 (sc-8204), goat anti-mouse osteopontin (AF808; R&D Systems), and rabbit anti-mouse osteocalcin (ab14173). These immunofluorescence protocols were applied using secondary antibodies: Daylight 488 donkey anti-Rabbit (Biolegend). Bone samples were collected from male and female mice at different time points.

Micro-CT

The tibias were scanned with micro-CT (MicroXCT-400; Xradia) with isotropic voxel dimensions ranging from 50 to 0.7 μm. The image data were subsequently quantified using a MicroView (3D Volume Viewer and Analysis Software). Two-dimensional images were used to generate 3-dimensional reconstructions and to calculate morphometric parameters defining trabecular bone mass and microarchitecture. These include bone mineral density (BMD), bone volume:tissue volume ratio (BV:TV), trabecular thickness (Tb.Th), trabecular number (Tb.N), and trabecular separation (Tb.Sp). Measurements were done in the 1.47 mm^3 volume (0.7 × 2.1 mm) located at 0.2 mm away from the growth plate of the distal end of tibia. Male mice were used.

Statistics

Differences between groups were evaluated by the Student *t* test or 2-way analysis of variance (ANOVA) assay. Data are expressed as mean ± SD or mean ± SEM, as indicated, and were considered statistically significant if *P* values were ≤.05.

Results

Enhanced CD34 expression on HSCs of FVIIIKO mice

To evaluate the potential regulatory role of FVIII on the HSC compartment in the BM, we initially analyzed by FACS the proportion

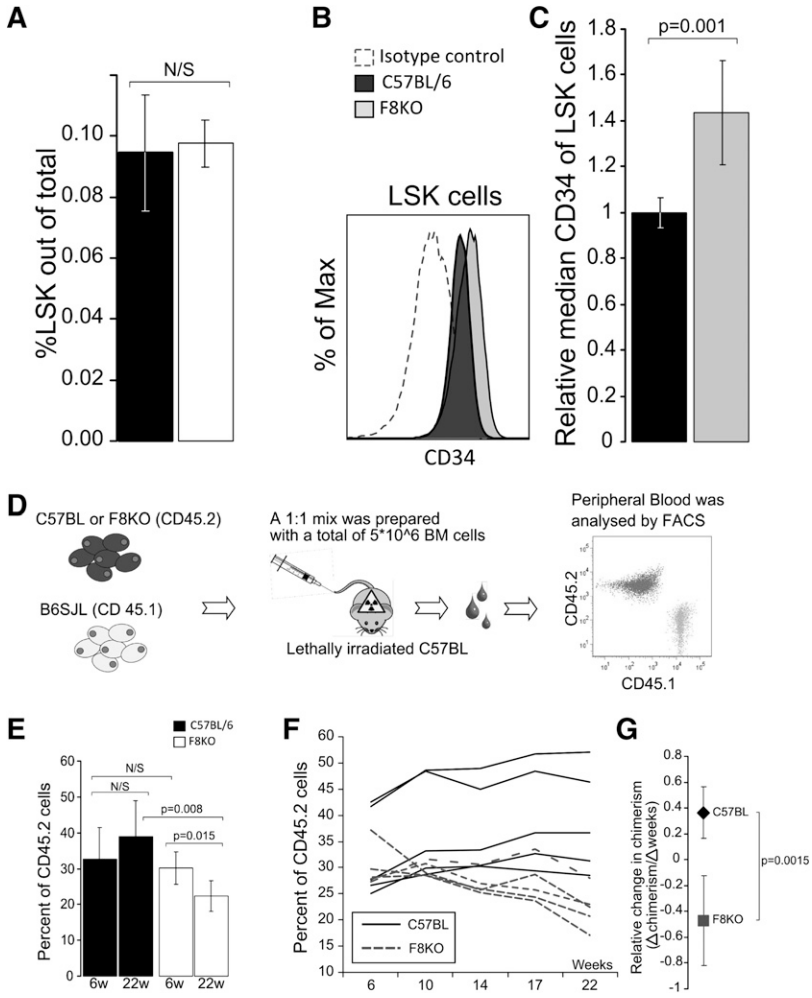

Figure 1. LSK cell levels in the BM of FVIIIKO vs wild-type (WT) mice. (A) Percentage of LSK cells in FVIIIKO (white) compared with WT (C57BL/6) mice (black) (0.976% ± 0.007% vs 0.946% ± 0.019% (n = 10, P = .671). (B) Representative FACS histograms comparing isotype control staining to CD34 staining on C57BL and FVIIIKO LSK are shown. (C) In 4 independent experiments, a total of 8 C57BL/6 and 7 FVIIIKO samples were stained for CD34 and the data analyzed as follows: first, the average CD34 median of the C57BL samples in each experiment was calculated. This value was then used as a reference for comparison against individual median CD34 values in the same experiment (ie, individual median of each mouse was divided by the average median staining of the C57BL group in the same experiment). FVIIIKO mice (gray) exhibited a significantly higher value (1.43 ± 0.226, N = 7) compared with the median value of C57BL (black) (1.0 ± 0.067, N = 8), $P < .001$. Error bars are means ± SD. (D-G) FVIII KO HSCs exhibit similar short-term but reduced LTR capacity. (d) Schematic representation of the competitive repopulation assay. Donor-type chimerism was defined by FACS in each recipient, and the average level was calculated based on the values found in the 6 recipients of every individual donor. In control experiments, the BM mixture was composed of similar numbers of B6SJL (CD45.1) and C57BL (CD45.2) WT BM cells. (E) Chimerism levels at 6 and 22 weeks after transplantation of C57BL/6 BM (black) and FVIIIKO BM (white). (F) Chimerism levels at different time points after transplantation of FVIIIKO BM (dashed line) and C57BL BM (black). Each line is based on the average values found in 6 recipients receiving BM from the same donor. Total number of mice was 30. (G) Average linear trend line slopes of donor-type chimerism over time in mice receiving FVIIIKO BM (square) vs mice receiving C57BL/6 BM (diamond). Error bars are means ± SD (n = 30 mice).

of the $Lin^-Sca^+Kit^+$ (LSK) population within HSCs. LSK cells are defined as $Sca1^+cKit^+$ cells within the Lin^- population. As can be seen in Figure 1A, the LSK percentage in FVIIIKO BM was not significantly different from that found in C57BL/6 mice. Considering that FVIIIKO mice also exhibit similar numbers of nucleated BM cells (data not shown), it seems that the absolute number of LSK cells remains unchanged. Likewise, no differences were found when different Lin^+ cell subpopulations were examined (data not shown).

To further assess the composition of the LSK population in FVIIIKO mice, the relative CD34 expression was determined by FACS analysis. CD34 expression is known to be elevated on short-term HSCs (ST-HSCs), compared with long-term HSCs (LT-HSCs).[14] As can be seen in Figure 1B-C, the median intensity of CD34 staining was significantly higher on the LSK population of FVIIIKO mice compared with that found in WT C57BL/6 mice. These results indicate that the FVIIIKO LSK cells might reflect a population at a more differentiated stage with reduced repopulating activity.

BM of FVIII KO mice exhibits enhanced short-term and reduced long-term hematopoietic repopulating activity

Based on the indication that FVIIIKO mice might exhibit reduced levels of LT-HSCs, we further tested the BM cells of these mice for their LTR capacity when transplanted into lethally irradiated mice. To that end, we transplanted competitively FVIIIKO BM cells expressing the CD45.2 antigen together with B6SJL BM cells expressing CD45.1 into lethally irradiated B6SJL mice at a 1:1 ratio (both strains are on C57BL/6 background and differ only in the CD45 alleles). Transplantation of $CD45.2^+$ BM cells from WT C57BL/6, together with B6SJL BM cells at a 1:1 ratio, was performed as control (Figure 1D).

Chimerism was determined by FACS analysis of donor-derived CD45.2 cells in the PB every month during a 22-week follow-up period, to allow sufficient time period for the exhaustion of the ST-HSC population (Figure 1E-F).

As can be seen in Figure 1E, depicting a typical experiment of 3 independent experiments, marked reduction in the LTR capacity of FVIIIKO was revealed. Thus, while at 6 weeks posttransplant, FVIIIKO BM exhibited similar chimerism levels (30.0% ± 4.5%) to that of WT C57BL/6 BM (32.7% ± 8.6%), marked reduction in chimerism was detected at the end of the 22-week period only in recipients of FVIIIKO donor BM (22.2% ± 4.4%), while recipients of WT C57BL/6 donor BM was not significantly changed (38.9% ± 9.9%) (n = 5, P = .008). This decline in chimerism found in the former mice, gradually proceeded over time, as indicated by the negative slope of −0.47 ± 0.34 (Δchimerism/Δweeks), while recipients of C57BL/6 BM exhibited a positive correlation of 0.36 ± 0.19 (Δchimerism/Δweeks) (n = 5, P = .0015) (Figure 1G). These data are in line with the higher expression of CD34 on HSCs of FVIIIKO mice, and strongly suggest that these mice are relatively depleted of LT-HSCs.

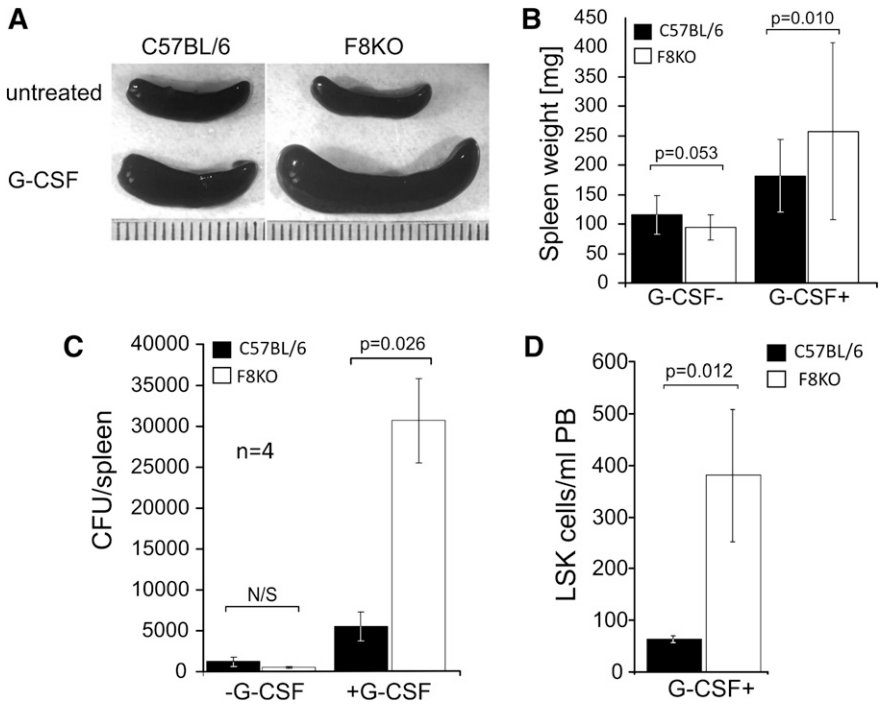

Figure 2. G-CSF–induced splenomegaly and LSK cell mobilization is enhanced in FVIIIKO mice. (A) Macroscopic view of selected spleens of FVIIIKO and C57BL/6 mice either with or without 7 days of G-CSF treatment. (B) Average spleen weight (mg) of C57BL/6 (left) and FVIIIKO (right) mice in the presence or absence of G-CSF treatment (2-way ANOVA, $P < .01$). (C) Number of CFUs before and after G-CSF treatment in the spleen of FVIIIKO (white) or C57BL/6 mice (black). (D) Number of LSK cells in PB of control and G-CSF–treated splenectomized FVIIIKO and C57BL/6 mice. Error bars are means ± SD.

FVIIIKO mice are more susceptible to G-CSF stimulation

Considering that G-CSF can induce proliferation of HSCs in the BM[15] followed by egress to the PB and marked splenomegaly,[11,16,17] this agent could potentially magnify and reveal HSC misbalance. Indeed, as depicted in Figure 2A-B, G-CSF–treated FVIIIKO mice exhibited a significantly enlarged spleen (316 ± 136 mg, n = 25) compared with their WT counterparts (181 ± 61, n = 32, 2-way ANOVA, $P < .05$). To establish the fact that spleen enlargement was the result of increased HSC number, we checked the number of colony-forming units (CFU-C) in each spleen. Indeed, spleens of FVIIIKO mice contained higher numbers of CFU-C (30 578 ± 5190 colonies per spleen, n = 4) compared with their C57BL/6 counterparts (5390 ± 1775 colonies per spleen, n = 4, $P = .026$), indicating that the observed growth was associated with growth of the HSC and progenitor cell compartment (Figure 2C). Since the spleen in the mouse is a primary hematopoietic organ that has resident HSCs,[18] we attempted to further test the effect of G-CSF on the BM alone by using splenectomized mice. As shown in Figure 2D, following G-CSF treatment, splenectomized FVIIIKO mice exhibited a more than threefold increase in LSK cells in their PB (380 ± 127 LSK cells per mL PB, n = 3), in comparison with splenectomized WT C57BL\6 mice (64 ± 6 LSK cells per mL PB, n = 3). These results suggest that FVIII KO HSCs are more prone to G-CSF mobilization and represent another indication of the disturbed balance existing within the HSC compartment of these mice.

Thrombin/PAR1 axis is associated with enhanced G-CSF stimulation in FVIIIKO mice

Apart from its coagulation attributes, FVIII has no other known physiological role. Thus, it is possible, that other downstream coagulation factors, in particular thrombin, affected by FVIII deficiency, are responsible for the observed distorted regulation of HSCs in FVIIIKO mice. To ascertain that FVIIIKO mice indeed exhibit reduced thrombin levels, we measured its levels in the plasma by the TGA (Figure 3A). FVIIIKO mice exhibited about a twofold decrease in peak plasma thrombin concentration compared with normal C57BL/6 mice (21.72 ± 5.8 nM vs 43.37 ± 6.4 nM, respectively). These results, showing that FVIIIKO mice are poor thrombin generators, strongly indicate that spontaneous generation of thrombin in vivo is likely lower in these mice.

The PAR1 is one of the major thrombin receptors and was previously shown to mediate thrombin noncoagulation activity in several cell types.[19]

Thus, based on the expected thrombin level results and by using the same G-CSF mobilization model that was used on the FVIIIKO mice, we further investigated the potential role of PAR1, in mediating enhanced G-CSF response. As can be seen in Figure 3B, similarly to FVIIIKO mice, PAR1KO mice exhibited enhanced levels of LSK cells in the PB after G-CSF treatment (766 ± 180 LSK cells per mL PB, n = 7) in comparison with C57BL mice (489 ± 189 LSK cells per mL PB, n = 5, $P < .005$). In a control experiment, mice with knockout of PAR2, a receptor for trypsin and not for thrombin, exhibited no enhancement of mobilization (488 ± 231, n = 6). Thus, the phenotype exhibited by FVIIIKO mice in which thrombin levels are markedly reduced, is also exhibited by PAR1KO mice, in which PAR1 signaling is absent altogether; these results support the suggestion that this phenotype could be partially mediated by thrombin via PAR1.

The relative contribution of stromal cells in the HSC niche to the HSC imbalance in PAR1KO mice

It is well established that the CXCL12/CXCR4 axis plays an important role in steady-state egress of HSCs as well as in G-CSF–induced mobilization.[20]

Considering the demonstration of Tzeng et al[21] in a conditional deletion model of CXCL12, that loss of stroma-secreted CXCL12 is associated with a reduced level of long-term quiescent stem cells, it was of interest to evaluate whether FVIII and PAR1KO mice exhibit reduced levels of CXCL12. As can be seen in Figure 3C, lower BM plasma levels of CXCL12 protein were measured both

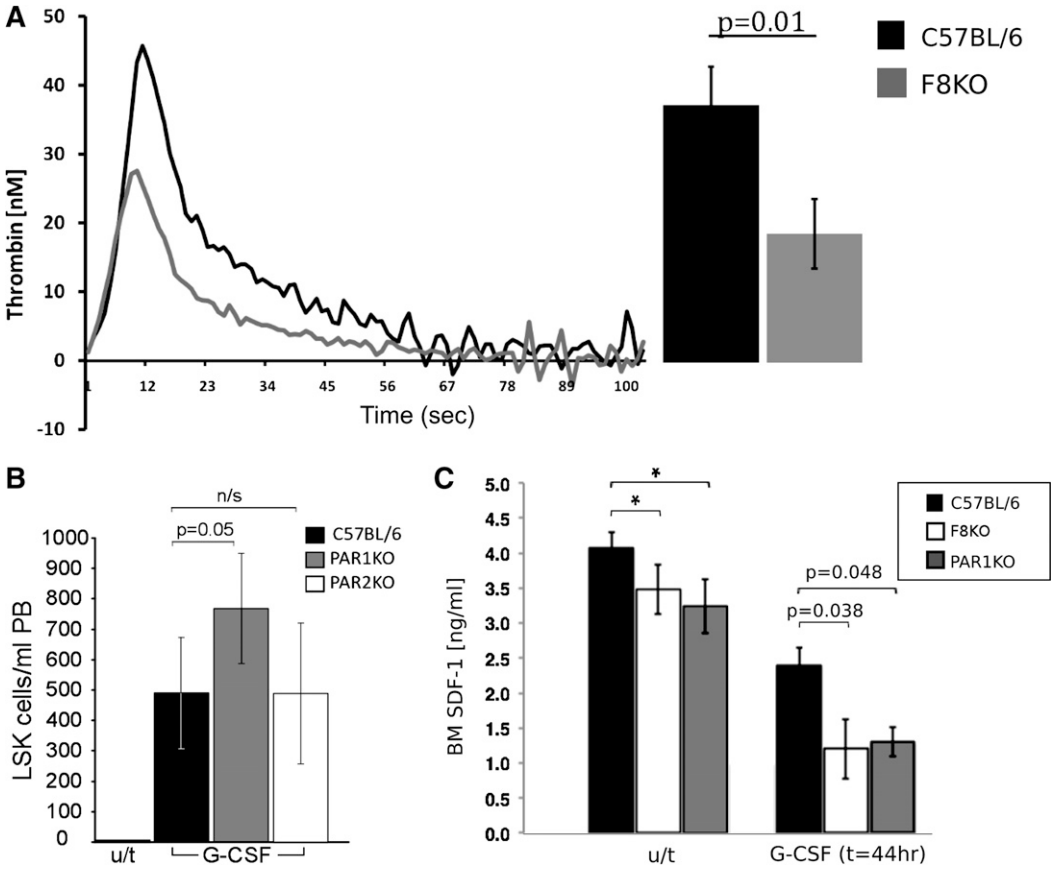

Figure 3. Thrombin\PAR1 axis is associated with enhanced G-CSF stimulation in FVIII KO mice. (A) Thrombin blood plasma levels (nM) in FVIIIKO (gray) and C57BL (black) mice at different time points as measured by the TGA. Summary of the results is depicted on the right (n = 4). (B) The number of LSK cells in PB of G-CSF–treated C57BL/6 (black), PAR1KO (gray), and PAR2KO (white) mice. (C) CXCL12 protein BM plasma levels detected by ELISA with and without G-CSF treatment in C57BL (black), FVIIIKO (white), and PAR1KO (gray) mice. Data are represented in (ng/mL); n = 12 per group.

in FVIIIKO (3.48 ± 0.35) and PAR1KO (3.24 ± 0.48) mice compared with C57BL/6 control (4.08 ± 0.21, 2-way ANOVA, $P < .05$). This trend was further enhanced in G-CSF–treated mice. Thus, significantly lower levels of CXCL12 protein were detected both in FVIIIKO (1.24 ± 0.42) and PAR1KO (1.32 ± 0.21) mice compared with WT C57BL/6 mice (2.04 ± 0.25) 44 hours following G-CSF administration.

Considering that mesenchymal stromal elements in the BM represent a major source of CXCL12, and given the fact that significantly lower levels of CXCL12 were detected in KO mice, we further speculated that the stroma might control, at least in part, the balance of LT-HSCs and ST-HSCs in the BM of WT mice through the thrombin/PAR1 axis. However, the imbalance of HSCs in PAR1 KO mice, revealed upon G-CSF treatment, could be as well attributed to the absence of PAR1 signaling on the HSCs themselves or to indirect signaling to stromal cells regulating the HSC pool.

To address this question, we prepared BM chimeras in which the BM was of PAR1KO origin and the recipients were WT C57BL mice or vice versa (Figure 4A). One month after BMT and upon confirmation of normal hematocrit recovery (data not shown), mice were treated with G-CSF and spleen weight (mg) was evaluated. As can be seen in Figure 4B, chimeras lacking PAR1 on their stromal cells only were more prone to G-CSF–induced splenomegaly (262 ± 43, n = 5, $P < .001$) compared with the control chimeras (157 ± 31, n = 10). A less potent but still significant enhancement was observed in the reciprocal chimeras lacking PAR1 on their hematopoietic cells (201 ± 42, n = 10, $P = .04$) (Figure 4B).

Thus, these results, together with the observed reduced CXCL12 BM plasma levels in FVIIIKO mice, suggest a predominant regulatory role for niche cells in HSC maintenance via thrombin/PAR1 axis, although some signaling of PAR1 on HSCs cannot be ruled out.

PAR1 is expressed by specific subpopulations of stromal niche cells

If indeed hematopoiesis is controlled in part through PAR1 on stromal elements, it was critical to evaluate PAR1 expression on potential niche components. PAR expression, including PAR1, was previously reported on mouse long bone and BM, while PAR1 expression was largely detected on BM stromal cells.[22]

More specifically, PAR1 was shown to be expressed on osteoblasts.[23] To further characterize potential PAR1-expressing stromal elements, we initially performed immunofluorescence staining of cryostat sections of femurs from C57BL/6 mice. As shown in Figure 5A, PAR1-positive osteoblast-like cells were situated as typical for osteoblasts, within the BM area near trabeculae and along the endosteum (Figure 5A-C). The latter is demarcated by staining for osteopontin (Figure 5A-B), a key component of the endosteal hematopoietic niche.[24] In addition, double staining for osteoclacin and PAR1 clearly verified that osteoblasts express PAR1 (Figure 5C), in line with Pagel et al.[23]

Recently, Nagasawa group described a unique multipotent $(PDGFR\alpha)^{+}Sca1^{-}$ mesenchymal stem cell (MSC) population residing

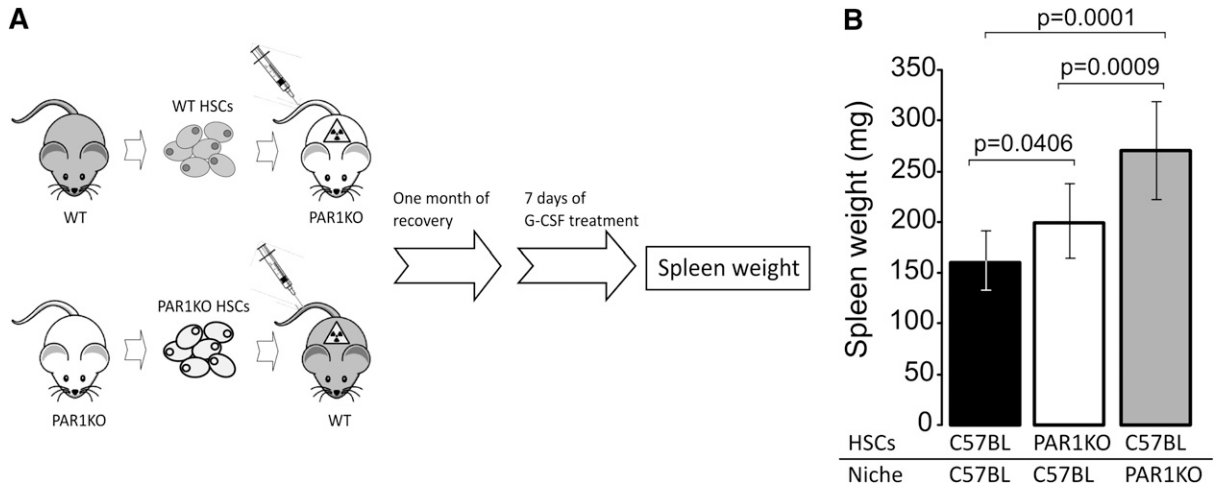

Figure 4. FVIIIKO and PAR1 KO mice exhibit impaired interaction between stroma cells and hematopoietic niche. (A) A scheme depicting the procedure in the assay used to distinguish between the roles of PAR1 on stromal cells vs PAR1 on HSCs. Host mice were lethally irradiated by split-dose total body irradiation (total of 10 Gy on day 3 and 4 Gy on day 1) and transplanted (day 0) with 5×10^6 donor cells. One month later, mice were mobilized by G-CSF for 7 days. (B) Spleen weight was examined for the 3 different chimeras tested as indicated. Bars represent average values ± SD.

in proximity to HSCs and expressing high levels of CXCL12[12] (accordingly, these cells were termed CXCL12-abundant reticular [CAR] cells). Importantly, they were able to demonstrate that CAR cell depletion has led to a marked reduction in lymphoid and erythroid progenitors and that HSCs from CAR cell–depleted mice were reduced in number.[12,13]

To further evaluate their potential relevance to the thrombin/PAR1 signaling pathway in the stroma, we attempted to identify these CAR cells by FACS, according to their unique PDGFRα$^+$ Sca1$^-$CD45$^-$CD31$^-$Ter119$^-$ phenotype and to define their PAR1 expression. As can be seen in Figure 5D, the median fluorescence intensity (MFI) of PAR1 expression on PDGFRα$^+$Sca1$^-$ stromal cells in C57BL/6 WT mice was 578.6 ± 53.5, significantly higher than the MFI for PAR1 staining in PAR1KO control mice (PAR1 staining of PAR1KO mice and isotype control staining of WT mice, yielded overlapping staining curves on FACS analysis with similar MFI levels of 397.0 ± 14.14 and 310.2 ± 22.1, respectively).

Similar documentation of PAR1 expression was attained by FACS analysis of CAR cells from mice expressing green fluorescent protein (GFP) under the CXCL12 promoter.[12] Thus, only the GFP-positive and not the GFP-negative fraction of the non-hematopoietic and nonendothelial CD45$^-$CD31$^-$Ter119$^-$ subpopulations were stained positively for PAR1 (Figure 5E). This selective PAR1 expression suggests that indeed PAR1 expression in the stroma compartment of the mouse BM is associated with CXCL12-expressing cells.

Recently, another unique subpopulation within the MSC population, namely Nestin-positive MSCs, was shown by Mendez-Ferrer et al[25] to express high levels of CXCL12 and to exhibit important HSC maintenance activity. In this work, these cells were shown to reside in the perivascular niche. Since Nestin cells also express CXCL12, it is possible that some of our PAR1-positive cells within the GFP-positive population were actually nestin-positive cells. We therefor repeated the previous experiment in mice expressing GFP under the nestin promoter.

Indeed, median PAR1 expression on these relatively rare cells in the BM was comparable to that exhibited by CAR cells, suggesting that both subpopulations could potentially be involved in the regulatory activity mediated through the FVIII/Thrombin/PAR1 axis.

Aberrant bone structure in FVIIIKO and PARKO mice

It has been established that the dynamic structure of the bone can influence hematopoiesis and HSC fate.[12,26] We therefore sought to determine whether disregulated HSCs, as in the case of FVIIIKO and PAR1KO, are associated with an aberrant bone structure. Figure 6A depicts bone collagen matrix staining (Sirius red), in WT, FVIIIKO, and PAR1KO newborn mice, and in 14-week-old mice. As can be seen, the collagen-outlined trabecular structures of adult compact bone were markedly distorted in FVIIIKO and PAR1KO mice as compared with WT control. Such differences were not observed in newborn bone, suggesting developmentally progressive character of changes in status of bone formation and remodeling in hemophilic and PAR1KO mice.

To determine the structural parameters of trabecular bone, we performed micro-CT analysis of the distal metaphysis of tibias harvested from 4-month-old mice. Quantification of the structural parameters of the tibial metaphysis are shown in Figure 6B. Thus, the BMD of FVIIIKO and PAR1KO mice was reduced by 7.1 ± 1.07 and 10.01% ± 1.86%, respectively ($P < .04$), compared with WT mice. Likewise, BV:TV and Tb.N were decreased by 57.13% ± 6.53%, 73.1% ± 4.7% in FVIIIKO ($P = .02$, $P < .001$), and 44.83% ± 15.2%, 37.11% ± 8.07% ($P = .03$, $P < .001$) in PAR1KO mice, respectively. In addition, Tb.Sp and Tb.Th in FVIIIKO mice were significantly increased by 304% ± 135% ($P < .001$) and 68.85% ± 17.1% ($P < .001$).

Collectively, these observations indicate that FVIIIKO mice exhibit decreased bone mass and compromised architecture of the bone. Similar pattern of malformed bone but in lesser extent was demonstrated for PAR1KO mice, suggesting that the thrombin/PAR1 axis plays an important role not only in hematopoiesis but also in regulating the interplay between HSC maintenance and the dynamic structure of the bone.

The significant aberration in bone mass could be attributed in part to reduced osteoblast activity as indicated in: "The relative contribution of stromal cells in the HSC niche to the HSC imbalance in PAR1KO mice," of the "Results" section, by our observation of reduced SDF-1 levels in BM plasma (Figure 3C). Indeed, this possibility was further substantiated by measuring serum osteocalcin level, a more specific marker of osteoblastic activity. Thus, as shown

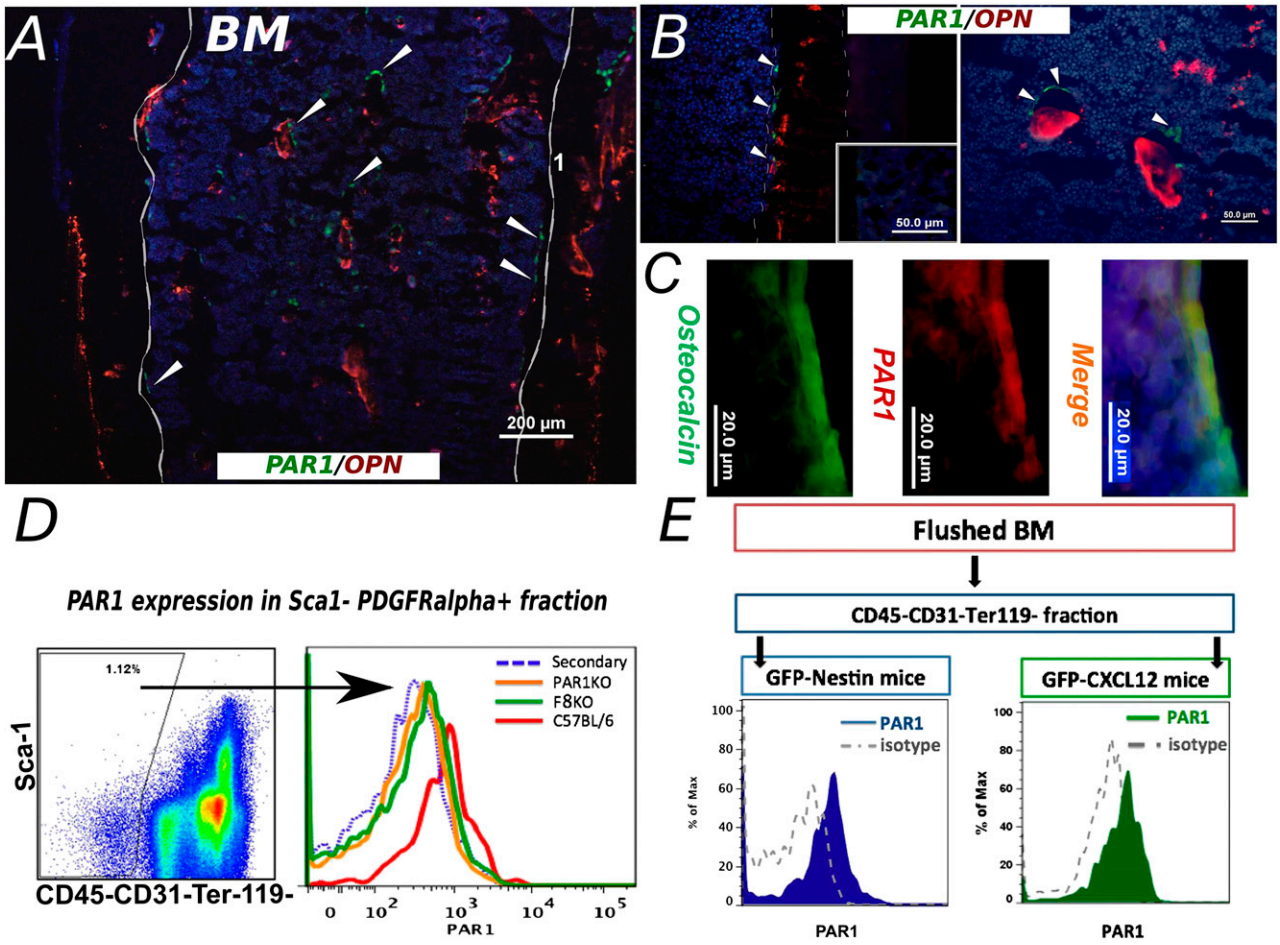

Figure 5. PAR1 expression by stromal niche cells. (A) A representative immunohistological staining of frozen femur from C57BL/6 mouse is shown. Sample was stained for Osteopontin (red) and PAR1 (green). Arrowheads point to some of the positive PAR1 staining. PAR1-positive cells were detected within the bone trabeculae, along the endosteum and as scattered cells areas inside the hematopoietic compartment (magnification, ×10). (B) Two larger magnification (×40) samples of staining for extracellular OPN together with membrane bound PAR1 staining are shown. Isotype control staining is depicted at the inset, using an irrelevant isotype-matched primary Ab for both PAR1 and OPN, followed by the secondary Ab used for the specific staining. OPN, osteopontin. (C) PAR1 specific expression on osteoblasts population is shown. Osteocalcin (green) is used as osteoblast specific intracellular marker. PAR1 is represented in red. Merge (yellow) demonstrates PAR1 expression on osteocalcin positive osteoblasts. Nuclei are denoted by Hoechst staining (blue). (D) FACS analysis of PAR1 expression on stromal cells. PAR1-positive signal was detected on $CD45^{-}CD31^{-}Ter119^{-}$ + $Sca1^{-}PDGFR\alpha^{+}$ subpopulation in C57BL/6 mice (red line). Similar cells of PAR1 KO mice were used as negative control (green line). (E) PAR1 expression was determined in GFP-CXCL12 and GFP-Nestin mice. Flushed fraction of BM was stained for CD45, CD31, and Ter119 and the negative fraction was examined for GFP signal. As can be seen, PAR1 expression was determined in both GFP CXCL12 (green) and GFP-Nestin (blue) mice. Isotype antibody staining was used as a negative control.

in Figure 6C, marked reduction was found in FVIIIKO and PAR1KO mice (45.42 ± 11.9 and 68.12% ± 15.94%, respectively) compared with the level exhibited by WT C57BL/6 mice (107.37 ± 26.02, $P < .05$).

Discussion

Our results demonstrate a novel regulatory role for the coagulation cascade in HSC maintenance and in regulating the bone structure. This regulatory role, initially discovered in FVIIIKO mice, is likely mediated, at least in part, through the FVIII/thrombin/PAR1 axis, as FVIIIKO mice exhibit reduced thrombin levels and PAR1KO mice, similarly to FVIIIKO mice, exhibit alterations in their HSC pool as well as in their bone structure. Significantly, our experiments in BM reciprocal chimeras suggest that the role of thrombin/PAR1 signaling can be predominantly attributed to the stromal cells, although a mild but significant impact of PAR1 signaling in HSCs was also suggested by these reciprocal chimeras.

The latter could be compatible with recent studies showing that activated protein C (APC) inactivates FV, FVIII, and thrombin, and that endothelial protein C receptor (EPCR)-bound APC induces PAR1 signaling.

This APC/EPCR/PAR1 pathway exerts multiple activities, including an antiapoptotic effect in HSCs,[27] antiinflammatory action[28] and antiendothelial barrier activation.[29] Recently, Suda's group[30] showed that $EPCR^{+}$ cells but not $EPCR^{-}$ cells in LSK stem cell population in fetal liver possess HSC characteristics. Furthermore they suggested that the ant-apoptotic effect is exerted by APC on $LSK/EPCR^{+}$ cells, indicating a possible involvement of the APC/EPCR/PAR-1 pathway in $EPCR^{+}$ HSC maintenance. In addition, HSC subset enriched in $CD150^{+}$ $EPCR^{+}CD48^{-}CD45^{+}$ of mouse fetal liver and adult BM cells were shown to be capable of repopulating irradiated congenic hosts for 4 months, producing clones of cells that can be serially transplanted.[31] Thus, the APC/EPCR/PAR1 pathway might be selectively expressed in LT-HSCs and not in the more cycling and differentiated ST-HSCs, and consequently lead to enhanced apoptosis of LT-HSCs. However, another study demonstrating very poor PAR1 cleavage by APC compared with thrombin

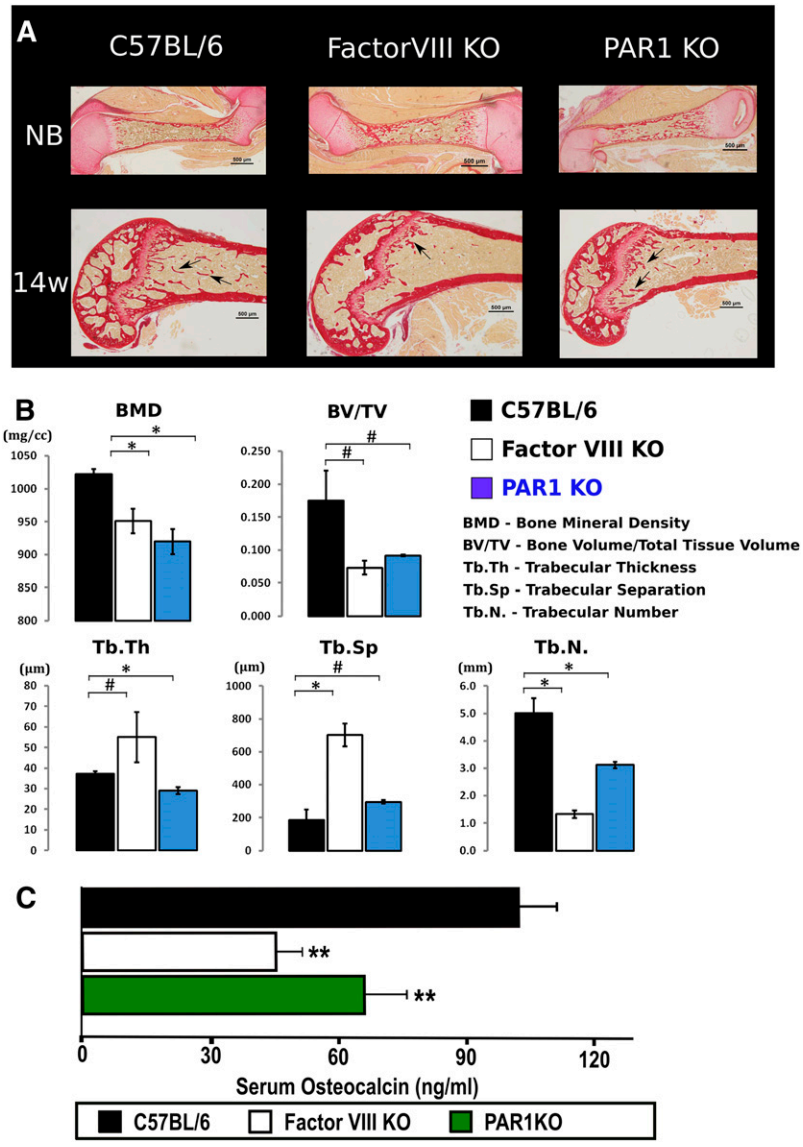

Figure 6. Aberrant bone structure in FVIIIKO and PAR1KO mice. (A) Bone connective tissue staining with sirius red for collagen synthesis is depicted. C57BL, FVIIIKO and PAR1KO are shown, respectively, at NB and 14 weeks of age. Arrows point to diminished amount of trabeculae in FVIIIKO and PAR1KO mice compared with C57BL control. NB, newborn. (B) Quantification of the structural parameters of the tibial metaphysis such as BMD, BV:TV, Tb.N, Tb.Th, and Tb.Sp. in C57BL (black), FVIIIKO (white), and PAR1KO (blue) are shown graphically. Graphs show mean value ± SD (#$P < .001$; *$P < .05$, n = 4/group). (C) Quantification of serum osteocalcin measured by ELISA. C57BL (black), FVIIIKO (white), and PAR1KO (green) are shown. Bars depict mean value ± SD (**$P < .05$, n = 10 per group).

(ie, by 4 orders of magnitudes),[32] indicates that a mechanism mediated through direct cleavage of PAR1 by thrombin is more realistic.

In line with our study in the reciprocal chimera indicating that stromal elements likely play a predominant role in mediating the observed phenotype of PAR1KO mice, examination of PAR1 staining either in conjunction with osteopontin or E-Cadherin staining suggests that most PAR1$^+$ cells in the BM are localized in the blood vessels or in perivascular sites while some can be also found in the endosteum area. The former is compatible with recently described leptin receptor positive, stem cell factor–producing stromal cells shown to be critical for HSC maintenance,[33] as well as CXCL12-abundant reticular cells[12] or nestin-expressing perivascular cells.[25] The latter 2 subpopulations, which secrete high levels of CXCL12, might overlap at least in part with the stem cell factor–producing cells. Our results showing that these subpopulations express PAR1, and that CXCL12 protein levels in BM plasma were reduced in FVIIIKO and PAR1KO mice, indicate that indeed our observed thrombin/PAR1 role in HSC maintenance might be mediated through any of these putative niche elements. Clearly, it is also tempting to link these putative niche cells to the major impact of the thrombin/PAR1 axis on the bone structure, as such MSC precursors were shown to be able to differentiate into osteoblasts and adipocytes.

However, the demonstration that cells expressing EYFP from Lepr-Cre, loxP-EYFP mice were not detected along the bone surface[33] indicates that lepr-expressing cells, which might largely equate to CAR cells, do not give rise to osteoblasts during normal development. This is consistent with the fact that adult bone lining osteoblasts are derived from osterix-expressing precursors in the embryonic perichondrium of developing bone during homeostasis.[34]

Thus, the Thrombin/PAR1 impact on bone remodeling could be largely mediated via PAR1-positive cells in the vicinity of the endosteum, in line with previous findings suggesting that thrombin likely exerts multiple effects upon osteoblasts, including induction of proliferation, inhibition of differentiation and apoptosis.[23]

Thrombin stimulation of primary WT mouse osteoblasts was also shown to be associated with increased expression of TGF β, COX-2, tenascin C, FGF1, FGF2, and IL-6, but not in PAR-1 null mouse osteoblasts.[23]

As shown in our present study, FVIIIKO mice exhibit lower generation of thrombin that in turn likely results in reduced PAR1 activation. Considering that osteoblasts express PAR1 as initially

suggested by Pagel et al[23] and also verified in the present study by costaining for PAR1 and osteocalcin, thrombin could exert its role in bone structure directly by controlling osteoblast activity. Indeed, this possibility was further indicated by our demonstration of reduced osteocalcin levels both in hemophilic and in PAR1KO mice. Furthermore, in parallel to the reduced activity of osteoblasts, the osteoclasts activity might be upregulated as shown by Wilson et al,[35] leading to increased bone degradation. Therefore, the initial altered bone metabolism in FVIII deficiency can predispose these mice toward enhanced egress and mobilization of HSCs to the periphery and might be responsible for the observed G-CSF–induced mobilization of LSK cells in FVIII and PAR1KO mice.

A possible pathway in which intracellular PAR1 signaling could directly affect niches of hematopoiesis is the phosphoinositide 3 (PI3) kinase signaling pathway that controls cell proliferation, growth, and survival. PI3 kinase is activated by integration of numerous upstream signals, one of which is the PAR1 activation of the G proteins αi and $\beta\gamma$. Critical downstream effectors of PI3-kinase signaling include the serine/threonine kinases Akt and mTorc1.[36] Additional potential pathway was indicated recently by Bar-Shavit et al[37] demonstrating an intracellular link between PAR1 and β-catenin stabilization independent of Wnt, but through the PAR1-induced $G\alpha_{13}$-disheveled axis.

Furthermore, it has been established that the dynamic structure of the bone can influence hematopoiesis and HSC fate.[26] Thus, conditional ablation of osteoblasts leads to progressive bone loss, followed by a decrease in the number of HSCs,[38] while increased osteoblast numbers caused by over expression of the parathyroid hormone was shown to enhance the number of HSCs.[39]

Our demonstration of disturbed balance in the HSC compartment in FVIIIKO mice could therefore be contributed in part to the observed altered bone metabolism in these animals, caused by reduced PAR1 signaling. Intriguingly, such indications of primary skeletal pathology were found in hemophilia A patients. Recent studies revealed lower BMD, increased urine calcium secretion, and reduced parathyroid hormone serum levels in children with hemophilia A.[40]

This chronic imbalance in BM microenvironment promotes an earlier onset of osteoporosis and chronic renal disease in these children. Further studies of BM biopsies from patients with hemophilia A might reveal whether indeed these patients exhibit reduced LT-HSC levels. Clearly, this might be of clinical relevance for those undergoing treatment involving stress to the HSC compartment that might lead to early exhaustion or to decline in numbers of true HSCs.[41]

In summary, our results reveal for the first time a novel regulatory role for the FVIII/thrombin/PAR1 axis in maintaining the LTR HSC pool as well as the fine balance between hematopoiesis and the bone structure. Our results in radiation chimera strongly suggest that this unique regulation is predominantly mediated through stromal cells. Further studies aiming at specific deletion of PAR1-positive stromal cells to define the more critical cell types in the HSC niche are warranted.

Acknowledgments

The authors thank Vlad Brumfeld (Department of Chemical Research Support) for assistance with micro-CT, and Prof Tsvee Lapidot and Shiri Gur-Cohen for valuable discussions.

This work was supported by the Israeli Science Foundation (grant no. 684/09).

Authorship

Contribution: A.A. and Y.N. designed and performed research, collected, analyzed, and interpreted data, performed statistical analysis, and wrote the manuscript; E.S., C.R., Y.Z.K., I.M., L.Y., D.H., and D.T.-Y. performed research and collected data; G.R. and U.M. designed research and contributed vital new reagents or analytical tools; T.N. and P.S.F. contributed vital new reagents or analytical tools; and Y.R. designed research, analyzed data, and wrote the paper.

Conflict-of-interest disclosure: The authors declare no competing financial interests.

Correspondence: Yair Reisner, Department of Immunology, Weizmann Institute of Science, Herzel St 1, Rehovot, Israel, 76100; e-mail: Yair.reisner@weizmann.ac.il.

References

1. Conlon I, Raff M. Size control in animal development. *Cell.* 1999;96(2):235-244.
2. Aronovich A, Tchorsh D, Katchman H, et al. Correction of hemophilia as a proof of concept for treatment of monogenic diseases by fetal spleen transplantation. *Proc Natl Acad Sci USA.* 2006; 103(50):19075-19080.
3. Dor FJ, Gollackner B, Cooper DK. Can spleen transplantation induce tolerance? A review of the literature. *Transpl Int.* 2003;16(7):451-460.
4. Aronovich A, Tchorsh D, Shezen E, et al. Enhancement of pig embryonic implants in factor VIII KO mice: a novel role for the coagulation cascade in organ size control. *PLoS ONE.* 2009; 4(12):e8362.
5. Stanger BZ, Tanaka AJ, Melton DA. Organ size is limited by the number of embryonic progenitor cells in the pancreas but not the liver. *Nature.* 2007;445(7130):886-891.
6. Dzierzak E, Speck NA. Of lineage and legacy: the development of mammalian hematopoietic stem cells. *Nat Immunol.* 2008;9(2):129-136.
7. Marley SB, Lewis JL, Gordon MY. Progenitor cells divide symmetrically to generate new colony-forming cells and clonal heterogeneity. *Br J Haematol.* 2003;121(4):643-648.
8. Zhang J, Niu C, Ye L, et al. Identification of the haematopoietic stem cell niche and control of the niche size. *Nature.* 2003;425(6960):836-841.
9. Kaushansky K. Lineage-specific hematopoietic growth factors. *N Engl J Med.* 2006;354(19): 2034-2045.
10. Kaushansky K. Thrombopoietin. *N Engl J Med.* 1998;339(11):746.
11. Platzbecker U, Prange-Krex G, Bornhäuser M, et al. Spleen enlargement in healthy donors during G-CSF mobilization of PBPCs. *Transfusion.* 2001;41(2):184-189.
12. Omatsu Y, Sugiyama T, Kohara H, et al. The essential functions of adipo-osteogenic progenitors as the hematopoietic stem and progenitor cell niche. *Immunity.* 2010;33(3): 387-399.
13. Morikawa S, Mabuchi Y, Kubota Y, et al. Prospective identification, isolation, and systemic transplantation of multipotent mesenchymal stem cells in murine bone marrow. *J Exp Med.* 2009; 206(11):2483-2496.
14. Osawa M, Hanada K, Hamada H, Nakauchi H. Long-term lymphohematopoietic reconstitution by a single CD34-low/negative hematopoietic stem cell. *Science.* 1996;273(5272):242-245.
15. Morrison SJ, Wright DE, Weissman IL. Cyclophosphamide/granulocyte colony-stimulating factor induces hematopoietic stem cells to proliferate prior to mobilization. *Proc Natl Acad Sci USA.* 1997;94(5):1908-1913.
16. Nilsson IM, Hedner U, Ahlberg Å. Haemophilia prophylaxis in Sweden. *Acta Paediatr.* 1976; 65(2):129-135.
17. Takamatsu Y, Jimi S, Sato T, Hara S, Suzumiya J, Tamura K. Thrombocytopenia in association with splenomegaly during granulocyte-colony-stimulating factor treatment in mice is not caused by hypersplenism and is resolved spontaneously. *Transfusion.* 2007;47(1):41-49.
18. Wolber FM, Leonard E, Michael S, Orschell-Traycoff CM, Yoder MC, Srour EF. Roles of spleen and liver in development of the murine hematopoietic system. *Exp Hematol.* 2002;30(9): 1010-1019.
19. Tsopanoglou NE, Maragoudakis ME. Thrombin's central role in angiogenesis and

pathophysiological processes. *Eur Cytokine Netw.* 2009;20(4):171-179.

20. Petit I, Szyper-Kravitz M, Nagler A, et al. G-CSF induces stem cell mobilization by decreasing bone marrow SDF-1 and up-regulating CXCR4. *Nat Immunol.* 2002;3(7):687-694.
21. Tzeng YS, Li H, Kang YL, Chen WC, Cheng WC, Lai DM. Loss of Cxcl12/Sdf-1 in adult mice decreases the quiescent state of hematopoietic stem/progenitor cells and alters the pattern of hematopoietic regeneration after myelosuppression. *Blood.* 2011;117(2):429-439.
22. Song SJ, Pagel CN, Campbell TM, Pike RN, Mackie EJ. The role of protease-activated receptor-1 in bone healing. *Am J Pathol.* 2005; 166(3):857-868.
23. Pagel CN, Song SJ, Loh LH, et al. Thrombin-stimulated growth factor and cytokine expression in osteoblasts is mediated by protease-activated receptor-1 and prostanoids. *Bone.* 2009;44(5): 813-821.
24. Nilsson SK, Johnston HM, Whitty GA, et al. Osteopontin, a key component of the hematopoietic stem cell niche and regulator of primitive hematopoietic progenitor cells. *Blood.* 2005;106(4):1232-1239.
25. Méndez-Ferrer S, Michurina TV, Ferraro F, et al. Mesenchymal and haematopoietic stem cells form a unique bone marrow niche. *Nature.* 2010; 466(7308):829-834.
26. Bianco P. Bone and the hematopoietic niche: a tale of two stem cells. *Blood.* 2011;117(20):5281-5288.
27. Balazs AB, Fabian AJ, Esmon CT, Mulligan RC. Endothelial protein C receptor (CD201) explicitly identifies hematopoietic stem cells in murine bone marrow. *Blood.* 2006;107(6):2317-2321.
28. Riewald M, Petrovan RJ, Donner A, Mueller BM, Ruf W. Activation of endothelial cell protease activated receptor 1 by the protein C pathway. *Science.* 2002;296(5574):1880-1882.
29. Esmon CT. The endothelial protein C receptor. *Curr Opin Hematol.* 2006;13(5):382-385.
30. Iwasaki H, Arai F, Kubota Y, Dahl M, Suda T. Endothelial protein C receptor-expressing hematopoietic stem cells reside in the perisinusoidal niche in fetal liver. *Blood.* 2010;116(4):544-553.
31. Kent DG, Copley MR, Benz C, et al. Prospective isolation and molecular characterization of hematopoietic stem cells with durable self-renewal potential. *Blood.* 2009;113(25):6342-6350.
32. Ludeman MJ, Kataoka H, Srinivasan Y, Esmon NL, Esmon CT, Coughlin SR. PAR1 cleavage and signaling in response to activated protein C and thrombin. *J Biol Chem.* 2005;280(13):13122-13128.
33. Ding L, Saunders TL, Enikolopov G, Morrison SJ. Endothelial and perivascular cells maintain haematopoietic stem cells. *Nature.* 2012; 481(7382):457-462.
34. Maes C, Kobayashi T, Selig MK, et al. Osteoblast precursors, but not mature osteoblasts, move into developing and fractured bones along with invading blood vessels. *Dev Cell.* 2010;19(2):329-344.
35. Wilson TJ, Nannuru KC, Singh RK. Cathepsin G recruits osteoclast precursors via proteolytic activation of protease-activated receptor-1. *Cancer Res.* 2009;69(7):3188-3195.
36. Coughlin SR. Protease-activated receptors in hemostasis, thrombosis and vascular biology. *J Thromb Haemost.* 2005;3(8):1800-1814.
37. Turm H, Maoz M, Katz V, Yin YJ, Offermanns S, Bar-Shavit R. Protease-activated receptor-1 (PAR1) acts via a novel Galpha13-dishevelled axis to stabilize β-catenin levels. *J Biol Chem.* 2010;285(20):15137-15148.
38. Visnjic D, Kalajzic Z, Rowe DW, Katavic V, Lorenzo J, Aguila HL. Hematopoiesis is severely altered in mice with an induced osteoblast deficiency. *Blood.* 2004;103(9):3258-3264.
39. Rashidi N, Adams GB. The influence of parathyroid hormone on the adult hematopoietic stem cell niche. *Curr Osteoporos Rep.* 2009;7(2): 53-57.
40. Ranta S, Viljakainen H, Mäkipernaa A, Mäkitie O. Hypercalciuria in children with haemophilia suggests primary skeletal pathology. *Br J Haematol.* 2011;153(3):364-371.
41. Ostronoff M, Ostronoff F, Campos G, et al. Allogeneic bone marrow transplantation in a child with severe aplastic anemia and hemophilia A. *Bone Marrow Transplant.* 2006; 37(6):627-628.